

Highly Strained Structure of a Four-Layer Deposit of Pd on Ni(110): A Coupled Theoretical and Experimental Study

J.-S. Filhol,^{1,3} M.-C. Saint-Lager,² M. De Santis,² P. Dolle,² D. Simon,^{1,3}
R. Baudoing-Savois,² J. C. Bertolini,³ and P. Sautet^{1,3}

¹Laboratoire de Chimie Théorique et des Matériaux Hybrides, École Normale Supérieure de Lyon,
46 allée d'Italie, 69364 Lyon Cedex 07, France

²Laboratoire de Cristallographie, CNRS, 25 avenue des Martyrs, 38042 Grenoble Cedex, France

³Institut de Recherches sur la Catalyse, CNRS, 2 avenue A. Einstein, 69626 Villeurbanne Cedex, France

(Received 17 April 2002; published 17 September 2002)

The structure of a four monolayer deposit of Pd on Ni(110) has been determined by a combination of x-ray diffraction experiments and density-functional theory calculations. This Pd film presents, after annealing at 500 K, a $(N \times 2)$ reconstruction associated with a large enhancement of its catalytic activity. The N superstructure, along the dense $[1\bar{1}0]$ direction, comes from periodic edge dislocations initiated by a vacancy in the first Pd layer. In the perpendicular direction, the doubling of the period originates in a pairing-buckling displacement of the rows. This study evidences a new Pd atoms arrangement with quasi-four-fold hollow sites on the surface, which could play an important role in the exceptional catalytic activity.

DOI: 10.1103/PhysRevLett.89.146106

PACS numbers: 68.35.Bs, 61.72.Dd, 68.55.Jk, 71.15.Mb

Bimetallic surfaces have a great interest for several applications ranging from magnetism to heterogeneous catalysis [1]. In the latter field, particles combining two transition metal atoms have often shown an enhanced activity for catalytic reactions, compared to pure metals [2]. Recent experiments have shown that Pd ultrathin films on a Ni(110) substrate can present a strongly enhanced activity for the catalytic hydrogenation of butadiene, a doubly unsaturated hydrocarbon. The maximum activity, 2 orders of magnitude larger than for pure palladium, is obtained with a 4 ML (monolayer) Pd film annealed at 500 K [3].

Two reasons are generally put forward to explain the modified activity of bimetallic surfaces [4–7]: the specific geometry and the modified electronic structure. The determination of the atomic arrangement at the catalyst surface is, hence, a major step. In the case of the annealed 4 ML Pd deposits, STM images exhibit a periodic wavelike structure, with a parameter of about 20 Å long and perpendicular to the $[1\bar{1}0]$ direction of the Pd film [8]. Moreover, LEED patterns indicate a $(N \times 2)$ reconstruction; x-ray diffraction has given $N \simeq 10$ –12 and showed that the $(N \times 2)$ superstructure involves the whole Pd film and even concerns the Ni substrate [9]. The large misfit (10%) between the bulk lattice parameters of Pd and Ni induces a large compressive strain in the Pd film which reconstructs to partially relax it. On one hand, first x-ray analysis explained the doubled periodicity, according to a $P2mm$ symmetry, by a sequence of atomic planes with, alternatively, row pairing (horizontal displacements) and row buckling (vertical displacements) [9]. On the other hand, density functional theory (DFT) calculations of the 1 ML film indicate that the compressive stress can be released by the formation of periodic vacancies along the $[1\bar{1}0]$ row, which can generate a N period [10,11].

The high complexity of the 4 ML deposit arises from the large reconstruction unit cell, hence the huge number of parameters to manage in fitting the experimental data. Solving the structure calls for a collaborative effort between experimental and theoretical approaches. From the theoretical point of view, this structure is close to the limits of the systems that can be handled at the DFT level: the unit cell is composed of 190 atoms and 1900 electrons. Previous theoretical studies of metallic films have been devoted to monolayers [12], and there is little information on multilayer systems.

The experiments were carried out at the SUV station of the French CRG-IF beam line (BM32) of the European Synchrotron Radiation Facility (ESRF) at Grenoble. The chamber (base pressure : 2×10^{-10} mbar) allows simultaneous *in situ* x-ray diffraction and molecular beam deposition [13]. The Ni(110) substrate was cleaned by cycles of Ar sputtering and annealing at 850 °C. The Pd film was evaporated with a growth rate of 0.2 ML/min and then annealed at 500 K. The structure was determined by x-ray diffraction with photon energy at 18 keV with a grazing incidence angle. The truncation of a periodic crystal gives rise to a rodlike distribution of the scattered intensity perpendicular to the surface, with a maximum surface sensitivity away from the 3D Bragg peaks [14]. In the present case, a new set of rods, parallel to the substrate ones, appears corresponding to the $(N \times 2)$ reconstruction where N was found equal to 11.

The Ni bulk lattice parameter is $a = 3.523$ Å. The (110) rectangular surface mesh is described by $a/\sqrt{2}$ along the close-packed $[1\bar{1}0]$ (X), a along the $[001]$ direction (Y), and $a/\sqrt{2}$ perpendicularly to the surface (Z). For the (11×2) reconstruction, we have built a large superstructure unit cell with two rows of 11 Ni atoms. Accordingly, the fundamental rods of the Ni substrate are at multiples of

11 in H with K even. For palladium, the bulk lattice parameter is 3.89 Å; this corresponds to H close to 10 and K close to 1.8. For the 4 ML system, x-ray diffraction reveals no trace of superstructure at $K = 1.8$, which indicates a mean inter-row distance in the Pd film equal to that in the Ni substrate. This distance being 10% lower than in bulk Pd, the Pd film is strongly strained by the epitaxial stress. The reduction of the measured (HKL) intensities and the structural analysis were done using the Anarod package available from ESRF [15], which we modified to deal with the present complex reconstruction.

The calculations of the structure were performed using the plane-wave DFT code VASP [16]. The Pd deposit on Ni is represented by periodic slabs. In the growth direction, the slabs are formed by five layers of Ni and four layers of Pd and are repeated in a supercell geometry with at least 8 Å of vacuum between them. The three first Ni layers are maintained frozen to the Ni bulk sites and all the above Pd and Ni layers are allowed to relax. DFT calculations of the bulk lattice parameter yield 3.53 Å for Ni, close to the real value, but 3.97 Å for Pd, slightly larger than the real one (3.89 Å). Hence, the compressive stress for Pd at the interface will be somewhat overestimated in the calculations.

A previous study has shown that the epitaxial 1 ML deposit can release the stress by the creation of periodic vacancies in the Pd layer in the $[1\bar{1}0]$ direction [10]. In the same way, the 4 ML structure is expected to reconstruct in order to release a large part of the epitaxial stress. To investigate this potential reconstruction, we first studied a 11×1 unit cell, where the Pd stress release is allowed by the transition from 11 Ni atoms per row at the interface to 10 Pd at the surface. The optimization of this 4 ML system leads to a periodic edge dislocation, initiated at the interface by a vacancy in the first layer of Pd. The Burgers vector is in the $[1\bar{1}0]$ direction, one of the favored directions for dislocation in fcc metals, and dislocation lines run in the $[001]$ direction. The formation of this array of dislocation greatly increases the stability of the surface (134 meV by Pd atom) as compared to the purely 4 ML epitaxial film. This result is consistent with the Frank and van der Merwe model [17], which predicts dislocative relaxation in annealed epitaxial films for a misfit over 9%.

For the periodicity doubling in the $[001]$ direction of the $(N \times 2)$ reconstruction, the pairing and buckling mode deduced from x-ray data may lead to two different surface terminations: paired or buckled rows. We calculated a 1×2 unit cell with each of these two surface terminations. Both structures are more stable than the pure epitaxial deposit, the paired surface being, however, 107 meV more stable than the buckled one.

The 11×2 structure was calculated by combining the pairing-buckling mechanism, with a paired row termination and the previous 11×1 dislocative model. The optimal 11×2 calculated structure is shown in Fig. 1. It is 7 meV by Pd atom more stable than the 11×1 structure.

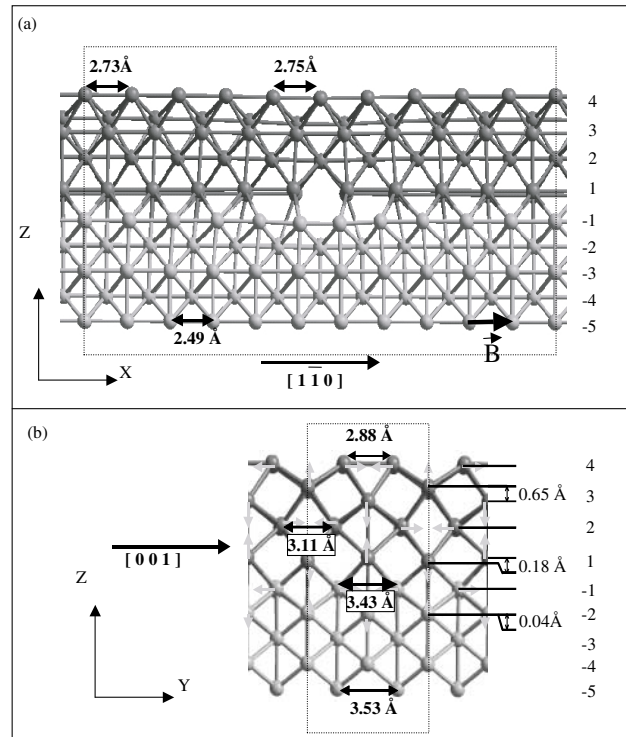


FIG. 1. Side views of the (11×2) structural model, (a) in the (X, Y) plane and (b) in the (Y, Z) plane. Pd planes are indexed from 1 to 4 and Ni ones from -1 to -5 . The Burgers vector \vec{B} associated with the dislocation is presented.

The total energy released from the 4 ML epitaxial deposit is huge with 141 meV by Pd atom.

In the final step, a set of parameters was designed in order to describe the main characteristics of the structure. This set was refined by fitting the x-ray experimental structure factors, starting from the value of the optimal DFT model. The best fitted x-ray structure factors are compared to the experimental ones in Fig. 2. The reliability of the fit is remarkably good owing to this very complex structure. Indeed, disorder was only accounted for by an anisotropic Debye Waller factor which does not include, for example, defects in the periodic dislocations arrays or stacking fault in the buckling/pairing plane sequence.

Let us now analyze the main features of this relaxed Pd film. The reconstruction in the $[1\bar{1}0]$ direction is clearly related to the atomic size misfit, which is accommodated here by a transition from 11 Ni atoms in the substrate (Ni-Ni distance: 2.49 Å) to 10 Pd atoms in the Pd layer 1 (Pd-Pd distance: 2.75 Å experimental, 2.81 Å calculated). At the interface, Pd layer 1 and Ni layer -1 , atoms are not equidistant along the X direction [Fig. 3(a)]. The structure can be viewed as a dislocation initiated at the interface by a Pd vacancy. Compared to the bulk distance, most Pd atoms are submitted to a compressive strain, except those near the vacancy which are under tensile strain. The distributions of interatomic distances deduced from fitting experimental data and from calculations are quite similar. In the Pd

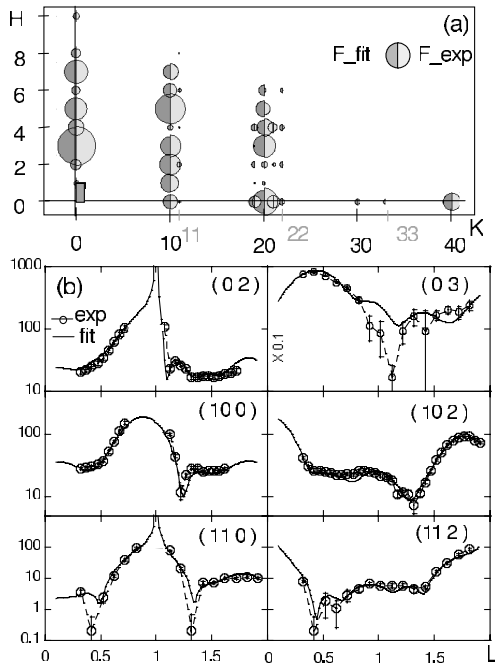


FIG. 2. Comparison of the fitted and experimental structure factors (a) in the plane $L = 0.32$ and (b) along the substrate rods (0 2), (11 0), and (11 2) and the superstructure rods (0 3), (10 0), and (10 2).

layer 1, it varies from 3.05 \AA near the vacancy to 2.59 \AA far away. Because of the strain at the interface, the displacements are just in opposite directions in Ni layer -1 and in Pd layer 1. The deformation in the Ni substrate side rapidly decreases with the distance from the interface [Fig. 3(b)].

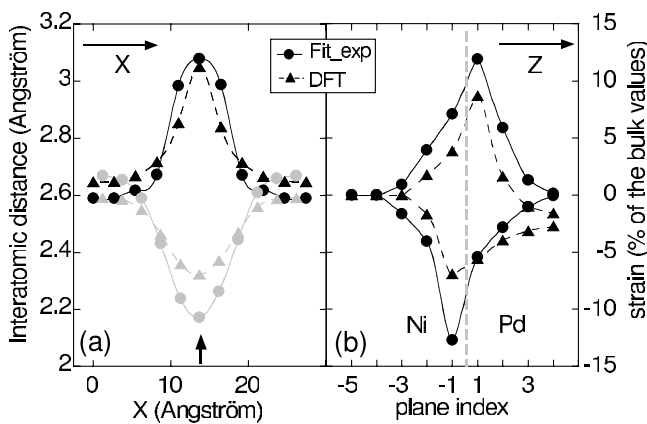


FIG. 3. (a) Variation of the interatomic distance along X for Ni layer -1 (gray) and Pd layer 1 (black). The arrow points to the vacancy. (b) Maxima of the tensile or compressive strain along X versus the plane index. For the Pd film, the positive values (tensile strains) correspond to atoms close to a vacancy plane, and the negative ones (compressive strains) to atoms in between two vacancies. The behavior is opposite for the Ni substrate. The bulk value is 2.49 \AA in the Ni side, 2.75 (fit-exp), and 2.81 \AA (DFT) in the Pd side.

The amplitude of the strain is slightly more pronounced in the experimental fit, with a deformation extending to the third Ni substrate layer (not included in the calculation).

In the outermost Pd layer 4, the experimental amplitude of the deformation along the rows vanishes. The remaining 2.5% compressive strain in the calculations is just an artifact arising from the (small) discrepancy between the DFT calculated and the real bulk Pd parameters. The $N = 11$ mesh periodicity along $[1\bar{1}0]$ (and the associated distance between periodic dislocations) ensures a bulk Pd-Pd distance at the surface, with a complete relaxation of the interfacial stress. Therefore, in the $[1\bar{1}0]$ direction, the dislocation-based relaxation mechanism is efficient, and Pd bulk distances are reached in the film fourth layer.

Things are completely different in the $[001]$ (Y) direction, perpendicular to the rows with a period doubling induced by a pairing-buckling type deformation [Fig. 1(b)]. Figure 4 shows the top and side views of the atomic arrangement given by the calculation and fitted from the experimental data, which are in excellent agreement. A striking aspect is the exceptionally large pairing deformation at the surface Pd layer 4, with an average shift of 0.34 \AA for each row. The result is the clear formation of a new bond with quasi-four-fold hollow sites at the (110) surface and an average Pd-Pd distance of 2.88 \AA . This represents a very large contraction of the inter-row spacing [35% compared to the case of a (110) surface of Pd]. A strong buckling amplitude (0.5 \AA) is induced in the Pd layer 3, the higher row being just below the larger gap in the pairing plane. Pairing and buckling alternate with a decreasing amplitude from the surface to the Ni substrate (let us emphasize that the pairing deformation in the Pd

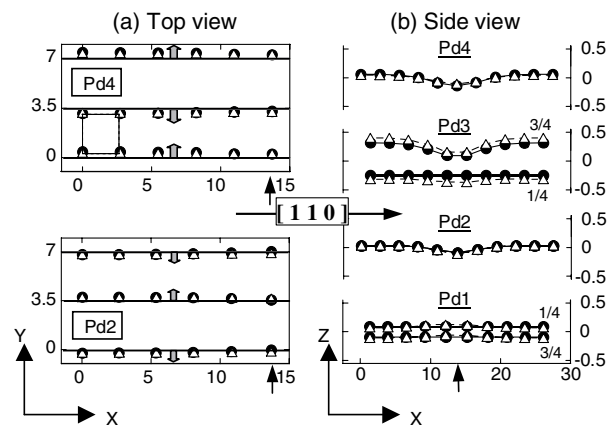


FIG. 4. Atomic positions fitted (circles) and DFT calculated (triangles); all the units are in \AA ; the black arrow points to the vacancy. (a) (X, Y) projection for the two Pd pairing planes, the scale is identical for X and Y (only half of the unit cell is shown along X), and the gray arrows give the shift direction relative to the reference Ni(110). (b) (X, Z) projection of the Z displacements relative to the averaged position of each Pd plane; in Pd layer 1 and Pd layer 3, the two rows, at $Y = \frac{1}{4}$ and $\frac{3}{4}$, are split but in opposite directions.

layer 2 is opposite to the one of the surface Pd layer 4). Pairing is still measurable in the Ni layer -1 with an inter-row spacing of 3.34 Å instead of 3.52 Å (pure Ni). Actually, the reconstruction along Y is not independent of that along X : the pairing is slightly modulated along the rows (about 7%) with a weaker pairing above dislocations.

In the [001] (Y) direction, the compression at the interface is kept up to the Pd layer 4, via the buckling/pairing row reconstruction, inducing a *complete change of the surface atom coordination*. In reaction to this lateral compression, the film expands in the vertical direction (e.g., Pd2-Pd4 spacing 3% larger) compared to Pd(110). This expansion does not fully compensate the lateral compression, and hence *the Pd atomic volume is reduced in the film by 7% (5%)* from the experimental (calculated) coordinates.

In addition, the rows are corrugated perpendicular to the surface, with a depression above the vacancies [Fig. 4(b)]. It is generated in the Pd layer 2, just above the vacancy, and propagates to the surface. The corrugation amplitude reaches 0.14 Å (10% of the interplane distance) and very nicely explains the periodic wavelike structure observed in the STM image [8].

Interdiffusion could also play an important role in the interfacial stress release mechanism. Experimentally, the fit is improved if we allow a partial occupation of the sites in Pd layer 1 by Ni atoms. In this buckled layer, the optimal configuration corresponds to the upper row mainly occupied by Pd atoms, and the lower one mainly by Ni. Beyond this layer, no significant interdiffusion has been evidenced.

Two different mechanisms are active for this 4 ML Pd film on Ni(110) substrate, in order to release the interfacial stress. Periodic vacancies are created along X at the interface, resulting in an efficient relaxation and a recovery of a bulklike parameter for Pd in the dense row direction already in the film fourth layer. The mechanism in the perpendicular direction is very different: the substrate mean inter-row distance is preserved up to the outermost layer 4 but with a very strong pairing-buckling reconstruction. This generates a very compact structure with a reduced atomic volume for Pd compared to the bulk. The main outcome, however, is the creation of a new surface structure on this highly strained Pd film. The pairing distortion is so large that new Pd-Pd bonds are created, resulting in quasi-four-fold hollow sites at this Pd(110) surface. This is completely unusual for (110) surfaces. For example, it is well known that hydrogen atoms can induce a pairing row reconstruction on a Pd(110) surface [18], topologically similar to the case shown here, but with

a much reduced amplitude and a spacing between paired rows of 3.23 Å, compared to 2.88 Å in our case. It can be suggested that such a new surface and coordination for Pd atoms at the film interface is an important insight for the understanding of the exceptional catalytic activity exhibited by this system.

This work was supported by the *Région Rhône-Alpes* under Contract No. 70006614 and by the computational resource center IDRIS (CNRS) under Contract No. 001064. We acknowledge the French CRG-BM32 (SUV) beam line staff for beam time and technical assistance.

-
- [1] F. Besenbacher, L. Pleth Nielsen, and P.T. Sprunger, in *The Chemical Physics of Solid Surfaces*, edited by D.A. King and D.P. Woodruff (Elsevier, Amsterdam, 1997), Vol. 8, Chap. 6.
 - [2] J.A. Rodriguez, *Heterog. Chem. Rev.* **3**, 17 (1996).
 - [3] P. Hermann, J.M. Guinier, B. Tardy, Y. Jugnet, D. Simon, and J.C. Bertolini, *J. Catal.* **163**, 169 (1996).
 - [4] J.-C. Bertolini, *Appl. Catal. A* **191**, 15 (2000).
 - [5] P. Sautet, in *Stress and Strain in Epitaxy: Theoretical Concepts, Measurements and Applications*, edited by M. Hanbücken and J.P. Deville (North-Holland, Amsterdam, 2001).
 - [6] B. Hammer and J. Nørskov, in *Advances in Catalysis*, edited by B.C. Gates and H. Knozinger (Academic, San Diego, 2000), Vol. 45, p. 71.
 - [7] M. Mavrikakis, B. Hammer, and J.K. Nørskov, *Phys. Rev. Lett.* **81**, 2819 (1998).
 - [8] L. Porte, M. Phaner-Goutorbe, J.-M. Guigner, and J.-C. Bertolini, *Surf. Sci.* **424**, 262 (1999).
 - [9] Full details on the experimental results and the data analysis will be reported elsewhere [M.C. Saint-Lager *et al.* (unpublished)].
 - [10] J.-S. Filhol, D. Simon, and P. Sautet, *Surf. Sci.* **472**, L139 (2001).
 - [11] J.-S. Filhol, D. Simon, and P. Sautet, *Phys. Rev. B* **64**, 085412 (2001).
 - [12] I. Meunier, G. Tréglia, J.-M. Gay, B. Aufray, and B. Legrand, *Phys. Rev. B* **59**, 10910 (1999).
 - [13] R. Baudoin-Savois *et al.*, *Nucl. Instrum. Methods Phys. Res., Sect. B* **149**, 213 (1999).
 - [14] I.K. Robinson, *Phys. Rev. B* **33**, 3830 (1986).
 - [15] E. Vlieg, *J. Appl. Crystallogr.* **33**, 401 (2000).
 - [16] G. Kresse and J. Hafner, *J. Phys. Condens. Matter* **6**, 8245 (1994); G. Kresse and J. Furthmüller, *Comput. Mater. Sci.* **6**, 15 (1996).
 - [17] F.C. Frank and J.H. van der Merwe, *Proc. R. Soc. London A* **198**, 216 (1949).
 - [18] V. Ledentu, W. Dong, P. Sautet, G. Kresse, and J. Hafner, *Phys. Rev. B* **57**, 12482 (1998).